Published in final edited form as:

J Alzheimers Dis. 2017 ; 60(3): 949–958. doi:10.3233/JAD-170269.

Brain Biomarkers in Familial Alzheimer's Disease Mouse Models

Yafit Kuttner-Hirshler[a,1], **Palamadai N. Venkatasubramanian**[b,1], **Joan Apolinario**[b], **Jacqueline Bonds**[a], **Alice M. Wyrwicz**[b], and **Orly Lazarov**[a,*]

[a]Department of Anatomy and Cell Biology, College of Medicine, The University of Illinois at Chicago, Chicago, IL, USA

[b]Center for Basic M.R. Research, Department of Radiology, NorthShore University HealthSystem, Evanston, IL, USA

Abstract

Alzheimer's disease (AD) is characterized by progressive loss of memory and cognitive deterioration. It is thought that the onset of the disease takes place several decades before memory deficits are apparent. Reliable biomarkers for the diagnosis or prognostication of the disease are highly desirable. Neural stem cells (NSC) exist in the adult brain throughout life and give rise to neural progenitor cells (NPC), which differentiate into neurons or glia. The level of NPC proliferation and new neuron formation is significantly compromised in mouse models of familial Alzheimer's disease (FAD). These deficits are readily detected in young adults, at 2–3 months of age, preceding amyloid deposition and cognitive impairments, which may indicate that impaired neurogenesis can be an early biomarker for cognitive deficits in AD. Recent studies suggest that NSC can be detected in live rodents, noninvasively, using proton magnetic resonance spectroscopy (^{1}H-MRS) signal at 1.28 ppm. Here we examined the use of ^{1}H-MRS for determining the extent of neurogenesis in the brains of FAD mice. We observed that the reduction in neurogenesis in the FAD mice as observed by immunohistochemistry, was not manifested by a reduction in the 1.28 ppm signal, suggesting that this marker is either not specific for neurogenesis or not sensitive enough for the detection of alterations in hippocampal neurogenesis in the brains of FAD mice.

Keywords

Alzheimer's disease; brain biomarkers; ^{1}H-MRS; mouse models; neurogenesis

INTRODUCTION

Currently, there are several biomarkers that are being tested for the diagnosis of Alzheimer's disease (AD), including positron emission tomography (PET), measuring brain amyloid-β (Aβ) levels using amyloid tracers such as Pittsburgh compound B (PIB), as well as Aβ and p-tau species in the cerebrospinal fluid and plasma of patients [1]. However, the specificity

*Correspondence to: Orly Lazarov, PhD, Professor, The University of Illinois at Chicago, Chicago, IL 60612, USA. Tel.: +1 312 355 0548; olazarov@uic.edu.

[1]These authors contributed equally to this work.

Authors' disclosures available online (http://j-alz.com/manuscript-disclosures/17-0269r1).

and predictive power of some of them are insufficient [2, 3]. Novel biomarkers with high diagnostic power are needed.

The purpose of this study was to identify a brain biomarker in live animals for the diagnosis of AD. Using immunohistochemistry and unbiased stereology we have shown previously that the level of neurogenesis in the subgranular zone of the dentate gyrus of the hippocampus (SGZ) and subventricular zone (SVZ) is reduced in young adult familial AD (FAD, APPswe/PS1 ΔE9) transgenic mice [4]. Similar observations have been described in other mouse models, such as 3XTg-AD [5] and others [6]. This may suggest that alterations in neurogenesis take place early in disease progression. Thus, if detectable in live mice, neurogenesis may be a biomarker for cognitive decline in AD. Previous studies suggest that neurogenesis can be exclusively detected by a 1.28 ppm signal of proton magnetic resonance spectroscopy (^{1}H-MRS) [7]. However, it is not clear if this biomarker can reflect the level of neurogenesis in pathological conditions, such as AD.

^{1}H-MRS provides a non-invasive way of assessing brain metabolites *in vivo*. Short echo-time proton MRS is capable of detecting several metabolites, including *N*-acetylaspartate (NAA), glutamate (Glu), glutamine (Gln), myo-inositol (mI), choline (Cho), and creatine (Cr). ^{1}H-MRS has been applied to the study of cognitive decline in humans. For example, in patients with amnestic mild cognitive impairment (aMCI) and AD, there is a decrease of NAA concentration and an increase of mI concentration. Other studies detected elevated ratio of mI to Cr levels [8]. Subjects with AD had most consistently decreased Glu/NAA or NAA/Cr in the parietal and occipital cortex. Other metabolite changes also were reported, such as decreased Glu as well as decreased Glu/Cr, Glu/mI, Glu/NAA, and NAA/Cr ratios compared to normal elderly controls [9]. Most of these studies have been performed using 3–4 Tesla scanners. Studies in mouse models of AD recapitulate these observations. Increased ratio of mI/Cr was observed in 3-month-old APPswe/PS1 ΔE9 mice and had a predictive power of 85% that increased as a function of age. The concentration of NAA was significantly lower at 8 months of age [10]. At 16 months of age, drop in level of NAA/Cr ratio in APPswe/PS1 ΔE9 mice was associated with the degeneration and intracellular deposition of thioflavine S-positive materials in hippocampal CA3 pyramidal neurons [11]. In transgenic mouse model of Tau pathology, rTg4510 mean hippocampal and cerebral cortex volumes were smaller than that in age-matched wild type and coincided with higher mI/tCr as well as with elevation of hyperphosphorylated tau, glial activation, and cortical and hippocampal neuronal loss [12].

Here, using ^{1}H-MRS, we examined the utility of the 1.28 ppm MRS signal in the dentate gyrus and subventricular zone, previously suggested to be a biomarker of adult neurogenesis [7]. In addition, we examined alterations in other brain metabolites in FAD mouse models in the search for a brain biomarker for AD.

MATERIALS AND METHODS

Animals and transgenic lines

Male APPswe/PS1 ΔE9 (n = 6, 6–7 months of age [13]), 3xTg mice (n = 6, 4 months of age, [14]), and age matched corresponding littermate wild type controls were used. All animal

experiments were approved by the University of Illinois at Chicago Institutional Animal Care and Use Committee (IACUC). Animals were maintained in standard conditions (14/10-h light/dark cycle) with full access to food and water *ad libitum*.

Proton MR spectroscopy

Anesthetized mice (isoflurane/oxygen 1.5–2.0%) were scanned on a Bruker Biospec 9.4T imaging spectrometer. Respiration rate was monitored and body temperature was maintained at 37°C during MR measurements. Localizer images were acquired using T_2-weighted RARE pulse sequence. Water suppressed proton spectra were acquired from 1 μl voxels located in the parietal cortex, dentate gyrus (DG), and subventricular zone (SVZ) using PRESS localization and VAPOR water suppression. TR/TE 2500 ms/20 ms, spectral width 4000 Hz, 4096 complex points, and 512 averages were used. Magnetic field homogeneity was optimized on each of the selected voxels using the field map method prior to acquiring the spectrum from that voxel. NAA, glutamate, glutamine, creatine, choline, mI, GABA and the signals at 1.28 ppm and 0.9 ppm were quantified using LCModel analysis and their levels expressed as ratio to total creatine in the same spectrum.

Neurosphere culture

Subventricular zone- or hippocampus-derived neural progenitor cells (NPCs) were isolated as previously described [15]. Adult male C57BL/6 mice (2–4 months of age, 3–4 per group) were sacrificed via isoflurane overdose followed by cervical dislocation. Their brains were immediately removed and dissected into two hemispheres. Hemispheres were then cut at approximately −0.94 mm relative to Bregma, according to an adult mouse brain atlas. Tissue samples were minced with a scalpel and incubated in 0.1% trypsin–EDTA (Invitrogen) for 7 min at 37°C. The enzymatic digestion was quenched with 3 parts 0.014% w/v trypsin inhibitor (Sigma) in HBSS (Life Technologies). After centrifugation, the pellet was resuspended in 1 ml of medium and mechanically triturated to disassociate the cells. The cells were then centrifuged at 700 rpm and resuspended in 500 μl of medium. Viable cells were counted on a hemocytometer using trypan blue exclusion (Sigma). NPCs were seeded at a density of 10,000 cells/cm^2 in non-tissue culture-treated 24-well plates (BD Biosciences) with 2 mL of medium per well containing 20 ng/mL human recombinant epidermal growth factor (EGF) and 10 ng/ml mouse recombinant FGF-2 (BD Biosciences). Medium consisted of DMEM/F-12 medium, supplemented with N2, B27, penicillin/streptomycin (Life Technologies), and 2 ρg/mL heparin (Sigma). Cells were incubated for 10 days in 37°C + 5% CO_2 to permit primary neurosphere formation. Cells were fed with growth factors every 3 days.

Stereotaxic injection of neurospheres

Mice were anesthetized using a mixture of ketamine and xylazine. The mice then had their heads shaved and wiped with 70% ethanol (EtOH). Animals were placed into the stereotaxic frame and a one-inch incision was made in the midline to reveal the Bregma. The scalp was then cleared of tissue and wiped with 30% hydrogen peroxide to dehydrate the scalp. A small hole was drilled at the coordinate site as measured from the Bregma according the mouse atlas of Paxinos and Franklin (2004). Neurospheres (1×10^6/1 μl) were stereotaxically injected unilaterally into the hippocampus of C57BL/6 mice (0.25 μl /min)

using the following coordinates: (anteroposterior, −3.0 mm; mediolateral, +2.0 mm; dorsoventral, −2.5 mm). Neurospheres were delivered using a 5 μl Hamilton syringe connected to a hydraulic system. The injection needle was then left in place for another minute. The needle was slowly retracted and the wounds were closed with sterile EZ-clips (Stoelting).

CldU regimen, immunohistochemistry, and stereology

5-Chloro-2′-deoxyuridine (CldU, 100 mg/kg body weight in 0.7% NaCl) was injected intraperitoneally 24 h before mice were sacrificed. Brains from per-fused mice were post-fixed in 4% paraformaldehyde for 3 days and stored in 30% sucrose at 4°C. The brains were then sectioned sagitally at 50 μm using a microtome and placed into cryoprotectant (23.8% glycerol, 28.5% ethylene glycol, 47.6% PBS v/v). Brain sections were blocked using 1× PBS containing 5% normal donkey serum and 0.05% Triton X-100 (Sigma). Sections were incubated for 72 h in primary antibodies [goat anti-doublecortin polyclonal (DCX, 1:400 Santa Cruz, Santa Cruz, California) and rat anti–BrdU (1:250, Accurate #OBT-0030, clone BU1/75) for the detection of CldU] followed by 2 h of blocking and 2 h of incubation in secondary antibodies. Slide mounting was performed using PVA/DABCO. Every sixth section was taken for stereological analysis as previously described [16, 17]. Briefly, quantification of immunostained sections was performed by Stereo Investigator using an optical fractionator (Micro-BrightField Bioscience). Immunostained sections were counted using the counting frames and sampling grid, which were set to 100 μm × 100 μm. The section thickness was averaged at 35 μm. Cells in the subgranular layer of the dentate gyrus were counted.

Statistics

Data are presented as means ± SE. Histological data were analyzed statistically by Student's *t* test. Metabolite levels calculated from LCModel analysis of MR spectra were compared between transgenic and wildtype control mice using *t*-Test assuming unequal variances. Results were considered statistically significant when $p \leq 0.05$.

RESULTS

1.28 ppm signal is detected in neurospheres

To examine whether the signal at 1.28 ppm is detected in the spectrum of neurospheres isolated from the adult brain, neurosphere cultures were prepared from the SVZ of adult mice as previously described [18]. Prior to imaging, neurospheres were washed and resuspended in DMEM only, to make sure that the spectrum reflects lipids of NPC rather than those present in the culture medium. Proton MR spectrum of neurospheres was obtained using the same pulse sequence and acquisition parameters used for *in vivo* spectra of the brain regions. The predominant signal in the neurosphere spectrum was at 1.28 ppm (Fig. 1A) as suggested by the relative intensity of the accompanying 0.9 ppm signal. In addition, resonances of lower intensity were also seen at 2.0 ppm, 2.35 ppm, 3.2 ppm, 3.6 ppm, and 3.8 ppm. In order to determine whether the 1.28 ppm peak is indicative of NPC *in vivo*, we compared the hippocampal spectrum of adult mice before and after transplantation of neurospheres into the hippocampus of adult mice. Water suppressed PRESS spectra were

acquired from a 1 μl voxel (1 mm × 1 mm × 1 mm) located in the DG of a wild type mouse brain before and after injection of neurospheres. After stereotactic injection of neurospheres, only the peaks at 1.28 ppm and 0.85 ppm were elevated (Fig. 1B, C), indicating that the elevated signals arise from the injected cells.

1.28 ppm and extent of neurogenesis in the brains of FAD mice

Having established that the 1.28 ppm peak reflects NPCs, we sought to determine whether the 1.28 ppm signal could be used for the detection of the extent of neurogenesis in FAD mouse models. For this purpose, we used two well-characterized FAD mouse models, the APPswe/PS1 ΔE9 [4, 13, 19–21] and the 3XTg-AD [14]. The examination of the spectra in two lines of FAD transgenic mice was intended to minimize the chance of transgene-related artifact. We compared the spectra from the two neurogenic regions (DG, SVZ) with that from a non-neurogenic brain region (cortex) of wild type and FAD mice. In all transgenic and nontransgenic groups we observed that the 1.28 ppm signal was more intense in the cortex than in neurogenic areas, the DG or SVZ, both of which are rich in newly formed neurons (Figs. 2A–C, 3A–C, G). Intragroup comparison of the cortical spectra revealed that the 1.28 ppm metabolite in the APPswe/PS1 ΔE9 and wild type was comparable (Figs. 2A, D, 3G). However, cortical signal of the 3XTg-AD was 4 times higher than the cortical signal of the wild type counterpart (Fig. 3A, D, G). Inter-genotype analysis revealed inconsistency concerning the intensity of the 1.28 ppm signal in the neurogenic areas. Specifically, in the SVZ, the 1.28 ppm signal was more intense in the transgenic compared to their corresponding wild type (Figs. 2B, E, 3B, E, G). However, in the hippocampus, no significant difference was found between the APPswe/PS1 ΔE9 and their corresponding wild type; whereas in the 3XTg-AD, intensity was greater than in the corresponding wild type (Figs. 2C, F, 3C, F, G). To try and understand the discrepancy, and examine whether this signal faithfully represents level of neurogenesis, we quantified hippocampal neurogenesis using unbiased stereology [4, 18]. We observed that the level of neuroblasts and immature neurons was reduced in the brains of APPswe/PS1 ΔE9 (Fig. 2G and Fig. 2H, I, respectively), and 3XTg-AD (Fig. 3H and Fig. 3I, J, respectively) mice compared to their wild type counterparts.

Metabolites in the brains of FAD transgenic mice

We next examined the extent of metabolites in the spectra in the range of 0–4.5 ppm in the cortex of APPswe/PS1 ΔE9 compared to wild type mice. We observed no difference in the intensity of most metabolites in the spectra, i.e., NAA, Cho, taurine (tau), inositol (Ins), Glu, and Gln (Fig. 4A). However, the intensity of GABA was significantly increased (Fig. 4A). This increase was apparent in the cortex, but not in the SVZ or hippocampus (Fig. 4B, C). In the SVZ we observed a significant increase in tau metabolite, whereas in the hippocampus, the levels of all metabolites detected were comparable.

Similar examination of the levels of metabolites in the spectra in the range of 0–4.5 ppm in the cortex of 3XTg-AD compared to their wild type counterparts revealed significant increases in the levels of Ins, Glu, and Gln (Fig. 5A). There was no difference in level of these metabolites in the SVZ (Fig. 5B) or the dentate gyrus of 3XTg-AD mice (Fig. 5C).

Notably, in the hippocampus, the level of metabolites was similar in transgenic compared to wild type mice in both the APPswe/PS1 ΔE9 and 3XTg-AD mice.

DISCUSSION

This study describes several observations concerning brain biomarkers in FAD mouse models. In the first part of this study we examined the ability to use the 1.28 ppm signal as a biomarker for neurogenesis in mouse models of FAD. In that regard, we first confirmed the appearance of the 1.28 ppm metabolite in the MR spectra of the neurosphere culture *in vitro*, and its increase following transplantation of neurospheres into the mouse brain. These results suggest that this metabolite represents, at least in part, neural progenitor cells. Since the $-(CH_2)_n-$ chain of fatty acids resonates at 1.2–1.3 ppm, the 1.28 ppm signal seen in neurospheres most likely is of lipidic origin. However, the exact nature of the molecule responsible for this signal needs further investigation. We found lack of consistency between the quantification of neurogenesis by stereology and the intensity of the 1.28 ppm signal, when comparing hippocampal neurogenesis in wild type and FAD-linked transgenic mice. This may raise several possibilities: (1) The methodology is not sensitive enough for the detection of differences in neurogenesis between the brains of FAD mice. The Manganas paper [7] compared the signal in the hippocampus versus the cortex of the same animal, while we compared the hippocampi of mice with different genotypes. The difference may lie in the quantity compared. In contrast to Manganas, where a neurogenic region was compared to a non-neurogenic one (“all or none”), in our case we expect a change of 20–30% in the number of NPCs between genotypes. It is possible that this method is not sensitive enough to capture this difference. (2) We used transgenic mice that exhibit brain pathology. Numerous changes take place in these brains, including changes in cellular phenotype. Thus, it is possible that under FAD-linked pathological conditions, this metabolite is present in other elements that do not exist in that form in the wild type, or that it represents additional cell types that may mask the effect. For example, the number of astrocytes and microglia is known to increase in both APPswe/PS1 ΔE9 and 3XTg-AD as a function of disease progression [14, 20]. Likewise, we cannot exclude the possibility of contribution of circulating peripheral inflammatory cells. (3) The 1.28 ppm signal represents a subpopulation of neurogenesis that was not captured in our stereological quantification. In that regard, it has been reported that 3xTg-AD mice accumulate ependymal cell-derived neutral lipids [22]. Mass spectrometric analysis of tissue sections revealed that there was a 2- to 27-fold increase in triglycerides in the SVZ of 3xTg-AD mice as a result of lipid metabolism alterations associated with hyper-activation of AKT signaling. While ependymal cells do not reside in the hippocampus, it is possible that the increase in triglycerides affects the spectra, and specifically, results in elevated 1.28 ppm signal seen in the SVZ and DG of 3xTg-AD. In such case, this signal does not reflect the number of neural progenitor cells and neurogenesis, but indicates impaired lipid metabolism in those regions associated with reduced neurogenesis. Thus, our results suggest that while the 1.28 ppm is enriched in NPCs, it may not be exclusive to this cell population and therefore is not a specific biomarker of neurogenesis in FAD models. It should be noted that a comparison between the 1.28 ppm observed following transplantation of NPCs and the extent of this metabolite in the FAD and wild type counterparts would not be appropriate for several reasons: (a) the

distribution of the neurogenic subpopulations *in vivo* is not faithfully represented *in vitro*. (b) not all subpopulations are present in the neurosphere culture. Particularly, it is reasonable to assume that the representation of quiescent neural stem cells *in vitro* is poor. (c) a comparison between stereology and singly dissociated count *in vitro* is challenging. (4) the 1.28 ppm metabolite in the cortex of wild type mice was greater compared to APPswe/PS1 ΔE9 mice, suggesting that this metabolite may not be specific to NPCs. In support of that, this metabolite is greater in the cortex than in the SVZ and DG of wild type mice. This discrepancy most likely arises from the poor spectral quality of cortical spectra when compared to DG and SVZ spectra, and contamination of the cortical voxel by extra-cortical lipids. A previous report has found that cortical spectra from the rat brain were generally of poor quality and many spectra had to be discarded and the remaining averaged before LCModel analysis could be used [23].

In the second part of this study, we identified several metabolites that are upregulated in the brains of FAD mice compared to wild type counterparts. Metabolites were differentially upregulated in the different brain areas of the FAD mice, suggesting a region-specific process rather than a global change in a specific metabolite. Furthermore, 3xTg-AD and APPswe/PS1 ΔE9 mice showed different patterns of metabolic alterations. Both FAD mice had the same metabolite profile in the DG as their wild type controls. A previous study investigating APPswe/PS1 ΔE9 mice by ^{1}H-MRS also found no variations in hippocampal metabolite levels at 8 months of age [24]. 3xTg-AD mice had elevated mI, glutamate, and glutamine in the cortex and no alterations in the SVZ. On the other hand, APPswe/PS1 ΔE9 mice had elevated GABA in the cortex and elevated taurine in the SVZ. mI is an astrocyte marker and osmolyte and has been reported to increase in AD patients [25]. Glutamate and glutamine are involved in excitatory neurotransmission and are also products of TCA cycle activity [25]. GABA is a primary inhibitory neurotransmitter and taurine has multiple biological functions, including osmoregulation and modulation of neurotransmitter function [26].

The 3XTg-AD and APPswe/PS1 ΔE9 mice were examined at different ages and disease stages, and exhibited different extent of pathology. Thus, the determination of an association between disease stage and specific metabolites by ^{1}H-MRS will require further analysis. In the 3XTg-AD mice, amyloid deposits are not apparent at 4 months of age. However, we cannot exclude the possibility that alterations in mI, Glu, and Gln may be due to upregulation of the ratio $A\beta_{42}/A\beta_{40}$ compared to wild type counterparts or other neuronal or glial changes that take place in the cortex at this stage. In the APPswe/PS1 ΔE9 mice, amyloid deposits are apparent at the examined time point of 6–7 months of age and may affect extent of metabolites.

In summary, our study suggests that the 1.28 ppm metabolite is insufficient for the specific identification and quantification of neurogenesis in the adult mouse brain, particularly in FAD. A set of neurogenesis-specific metabolites would enhance our ability to analyze the extent of neurogenesis in the brains of FAD mouse models.

Acknowledgments

This study was supported by NIH National Institute on Aging (NIA) 1RC1AG036208-01, R01AG03 3570 and R01AG033570-S2 (OL).

References

1. Weiner MW, Veitch DP, Aisen PS, Beckett LA, Cairns NJ, Green RC, Harvey D, Jack CR Jr, Jagust W, Morris JC, Petersen RC, Saykin AJ, Shaw LM, Toga AW, Trojanowski JQ. Alzheimer's Disease Neuroimaging Initiative. Recent publications from the Alzheimer's Disease Neuroimaging Initiative: Reviewing progress toward improved AD clinical trials. Alzheimers Dement. 2017; 13:e1–e85. [PubMed: 28342697]
2. Vlassenko AG, McCue L, Jasielec MS, Su Y, Gordon BA, Xiong C, Holtzman DM, Benzinger TL, Morris JC, Fagan AM. Imaging and cerebrospinal fluid biomarkers in early preclinical alzheimer disease. Ann Neurol. 2016; 80:379–387. [PubMed: 27398953]
3. Jack CR Jr, Bennett DA, Blennow K, Carrillo MC, Feldman HH, Frisoni GB, Hampel H, Jagust WJ, Johnson KA, Knopman DS, Petersen RC, Scheltens P, Sperling RA, Dubois B. A/T/N: An unbiased descriptive classification scheme for Alzheimer disease biomarkers. Neurology. 2016; 87:539–547. [PubMed: 27371494]
4. Demars M, Hu YS, Gadadhar A, Lazarov O. Impaired neurogenesis is an early event in the etiology of familial Alzheimer's disease in transgenic mice. J Neurosci Res. 2010; 88:2103–2117. [PubMed: 20209626]
5. Rodriguez JJ, Jones VC, Tabuchi M, Allan SM, Knight EM, LaFerla FM, Oddo S, Verkhratsky A. Impaired adult neurogenesis in the dentate gyrus of a triple transgenic mouse model of Alzheimer's disease. PLoS One. 2008; 3:e2935. [PubMed: 18698410]
6. Lazarov O, Mattson MP, Peterson DA, Pimplikar SW, van Praag H. When neurogenesis encounters aging and disease. Trends Neurosci. 2010; 33:569–579. [PubMed: 20961627]
7. Manganas LN, Zhang X, Li Y, Hazel RD, Smith SD, Wagshul ME, Henn F, Benveniste H, Djuric PM, Enikolopov G, Maletic-Savatic M. Magnetic resonance spectroscopy identifies neural progenitor cells in the live human brain. Science. 2007; 318:980–985. [PubMed: 17991865]
8. Kantarci K, Petersen RC, Przybelski SA, Weigand SD, Shiung MM, Whitwell JL, Negash S, Ivnik RJ, Boeve BF, Knopman DS, Smith GE, Jack CR Jr. Hippocampal volumes, proton magnetic resonance spectroscopy metabolites, and cerebrovascular disease in mild cognitive impairment subtypes. Arch Neurol. 2008; 65:1621–1628. [PubMed: 19064749]
9. Rupsingh R, Borrie M, Smith M, Wells JL, Bartha R. Reduced hippocampal glutamate in Alzheimer disease. Neurobiol Aging. 2011; 32:802–810. [PubMed: 19501936]
10. Chen SQ, Cai Q, Shen YY, Wang PJ, Teng GJ, Li MH, Zhang W, Zang FC. (1)H-MRS evaluation of therapeutic effect of neural stem cell transplantation on Alzheimer's disease in AbetaPP/PS1 double transgenic mice. J Alzheimers Dis. 2012; 28:71–80. [PubMed: 21955813]
11. Xu D, Vigneron D. Magnetic resonance spectroscopy imaging of the newborn brain–a technical review. Semin Perinatol. 2010; 34:20–27. [PubMed: 20109969]
12. Yang D, Xie Z, Stephenson D, Morton D, Hicks CD, Brown TM, Sriram R, O'Neill S, Raunig D, Bocan T. Volumetric MRI and MRS provide sensitive measures of Alzheimer's disease neuropathology in inducible Tau transgenic mice (rTg4510). Neuroimage. 2011; 54:2652–2658. [PubMed: 21035554]
13. Jankowsky JL, Slunt HH, Ratovitski T, Jenkins NA, Copeland NG, Borchelt DR. Co-expression of multiple transgenes in mouse CNS: A comparison of strategies. Biomol Eng. 2001; 17:157–165. [PubMed: 11337275]
14. Oddo S, Caccamo A, Shepherd JD, Murphy MP, Golde TE, Kayed R, Metherate R, Mattson MP, Akbari Y, LaFerla FM. Triple-transgenic model of Alzheimer's disease with plaques and tangles: Intracellular Abeta and synaptic dysfunction. Neuron. 2003; 39:409–421. [PubMed: 12895417]
15. Bonaguidi MA, Peng CY, McGuire T, Falciglia G, Gobeske KT, Czeisler C, Kessler JA. Noggin expands neural stem cells in the adult hippocampus. J Neurosci. 2008; 28:9194–9204. [PubMed: 18784300]

16. Demars MP, Hollands C, Zhao KD, Lazarov O. Soluble amyloid precursor protein-alpha rescues age-linked decline in neural progenitor cell proliferation. Neurobiol Aging. 2013; 34:2431–2440. [PubMed: 23683827]
17. Lazarov O, Demars MP, Zhao Kda T, Ali HM, Grauzas V, Kney A, Larson J. Impaired survival of neural progenitor cells in dentate gyrus of adult mice lacking FMRP. Hippocampus. 2012; 22:1220–1224. [PubMed: 22128095]
18. Gadadhar A, Marr RA, Lazarov O. Presenilin-1 regulates neural progenitor cell differentiation in the adult brain. J Neurosci. 2011; 31:2615–2623. [PubMed: 21325529]
19. Lazarov O, Robinson J, Tang YP, Hairston IS, Korade-Mirnics Z, Lee VM, Hersh LB, Sapolsky RM, Mirnics K, Sisodia SS. Environmental enrichment reduces Abeta levels and amyloid deposition in transgenic mice. Cell. 2005; 120:701–713. [PubMed: 15766532]
20. Lazarov O, Lee M, Peterson DA, Sisodia SS. Evidence that synaptically released beta-amyloid accumulates as extracellular deposits in the hippocampus of transgenic mice. J Neurosci. 2002; 22:9785–9793. [PubMed: 12427834]
21. Hu YS, Long N, Pigino G, Brady ST, Lazarov O. Molecular mechanisms of environmental enrichment: Impairments in Akt/GSK3beta, neurotrophin-3 and CREB signaling. PLoS One. 2013; 8:e64460. [PubMed: 23700479]
22. Hamilton LK, Dufresne M, Joppe SE, Petryszyn S, Aumont A, Calon F, Barnabe-Heider F, Furtos A, Parent M, Chaurand P, Fernandes KJ. Aberrant lipid metabolism in the forebrain niche suppresses adult neural stem cell proliferation in an animal model of Alzheimer's disease. Cell Stem Cell. 2015; 17:397–411. [PubMed: 26321199]
23. Park JH, Lee H, Makaryus R, Yu M, Smith SD, Sayed K, Feng T, Holland E, Van der Linden A, Bolwig TG, Enikolopov G, Benveniste H. Metabolic profiling of dividing cells in live rodent brain by proton magnetic resonance spectroscopy (^{1}H-MRS) and LCModel analysis. PLoS One. 2014; 9:e94755. [PubMed: 24819091]
24. Jansen D, Zerbi V, Janssen CI, Dederen PJ, Mutsaers MP, Hafkemeijer A, Janssen AL, Nobelen CL, Veltien A, Asten JJ, Heerschap A, Kiliaan AJ. A longitudinal study of cognition, proton MR spectroscopy and synaptic and neuronal pathology in aging wild-type and AbetaPPswe-PS1dE9 mice. PLoS One. 2013; 8:e63643. [PubMed: 23717459]
25. Lin A, Ross BD, Harris K, Wong W. Efficacy of proton magnetic resonance spectroscopy in neurological diagnosis and neurotherapeutic decision making. NeuroRx. 2005; 2:197–214. [PubMed: 15897945]
26. Govindaraju V, Young K, Maudsley AA. Proton NMR chemical shifts and coupling constants for brain metabolites. NMR Biomed. 2000; 13:129–153. [PubMed: 10861994]

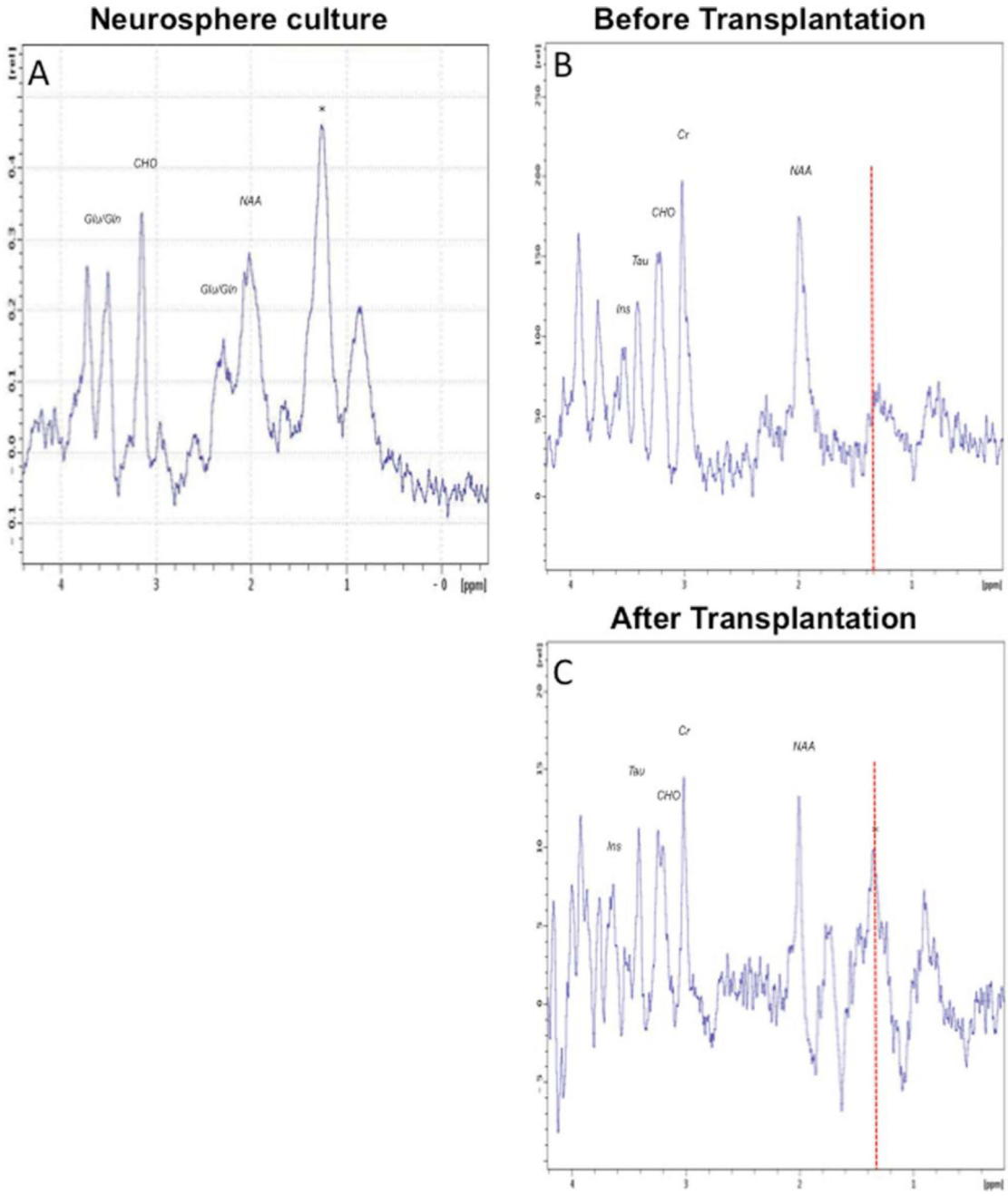

Fig. 1.

Examination of the 1.28 ppm metabolite in neural progenitor cells using ^{1}H-MRS. A) ^{1}H-MR spectra of neurospheres isolated from the adult mouse subventricular zone shows the 1.28 ppm metabolite (*) as the dominant signal. PRESS localized water suppressed spectrum was acquired from a 1 μl voxel. Resonances from NAA, Glu/Gln, and choline containing compounds are also seen in the spectrum of neurospheres. B, C) *In vivo* localized ^{1}H-MR spectra of mouse brain before (B) and after (C) injection of neurospheres. PRESS localized water suppressed spectra were acquired from a 1 μl voxel located in the dentate gyrus including the subgranular zone. The spectrum after cell injection shows enhanced

signal intensity at 1.28 ppm (*). This signal is characteristic of newly formed neuronal cells. Signals from NAA, Cr, choline containing compounds, taurine and inositol are seen at the same level before and after injection of neurospheres.

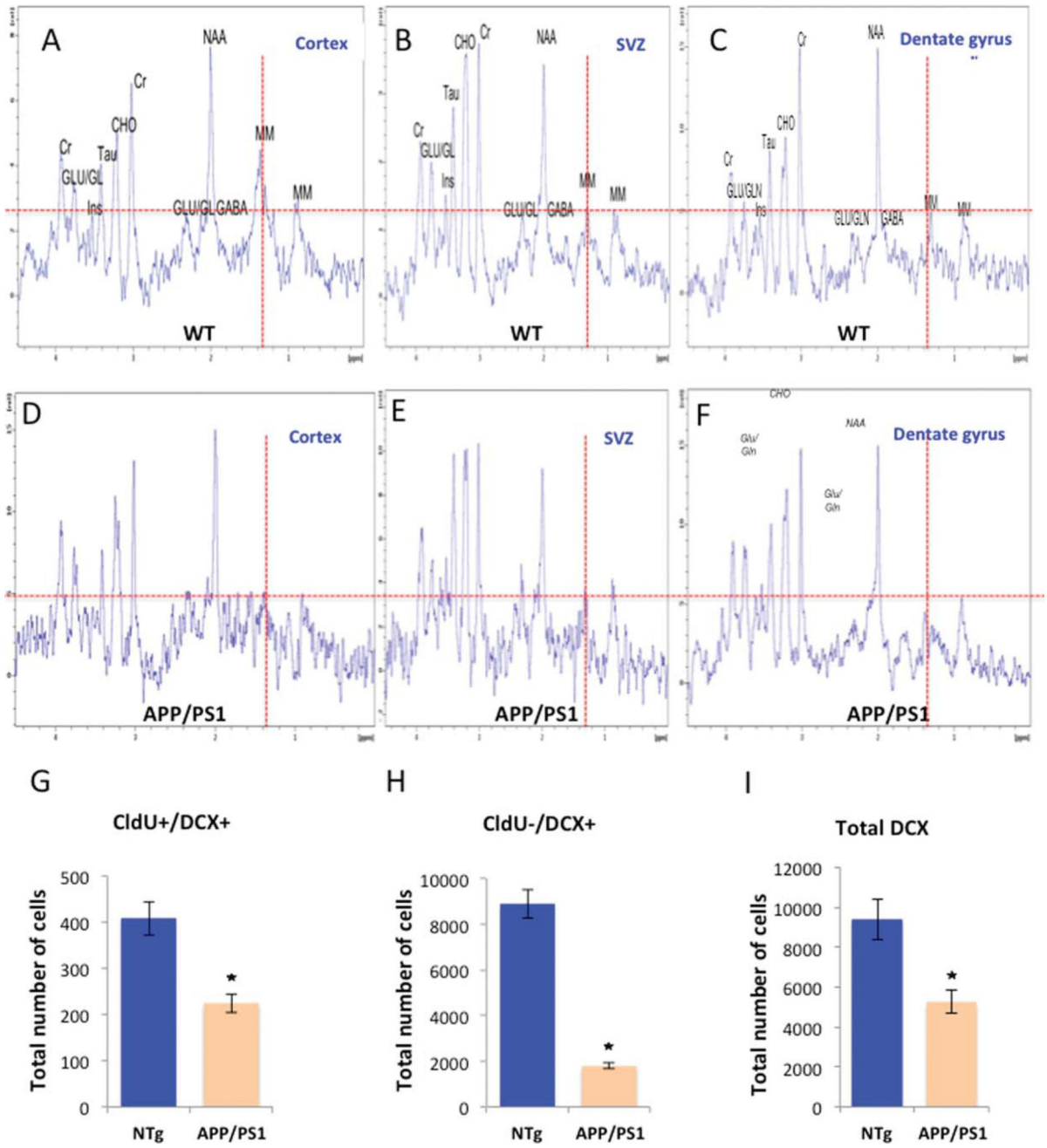

Fig. 2.

Level of the 1.28 ppm metabolite in the brains of APPswe/PS1 ΔE9 mice compared to level of neurogenesis by stereology. *In vivo* localized ^{1}H-MR spectra of mouse cortex (A, D), subventricular zone (B, E), and hippocampus (C, F) of wild type (A–C) and APPswe/PS1 ΔE9 (D–F) mice. (G–I) Extent of neurogenesis in the hippocampus of wild type and APPswe/PS1 ΔE9 mice using unbiased stereology (CldU, 5-Chloro-2′-deoxyuridine; DCX, doublecortin). The number of proliferating neuroblasts (CldU+/DCX+, G), immature neurons (CldU−/DCX+, H) and total newly forming neurons (total DCX, I) is reduced in the APP/PS1 mice.

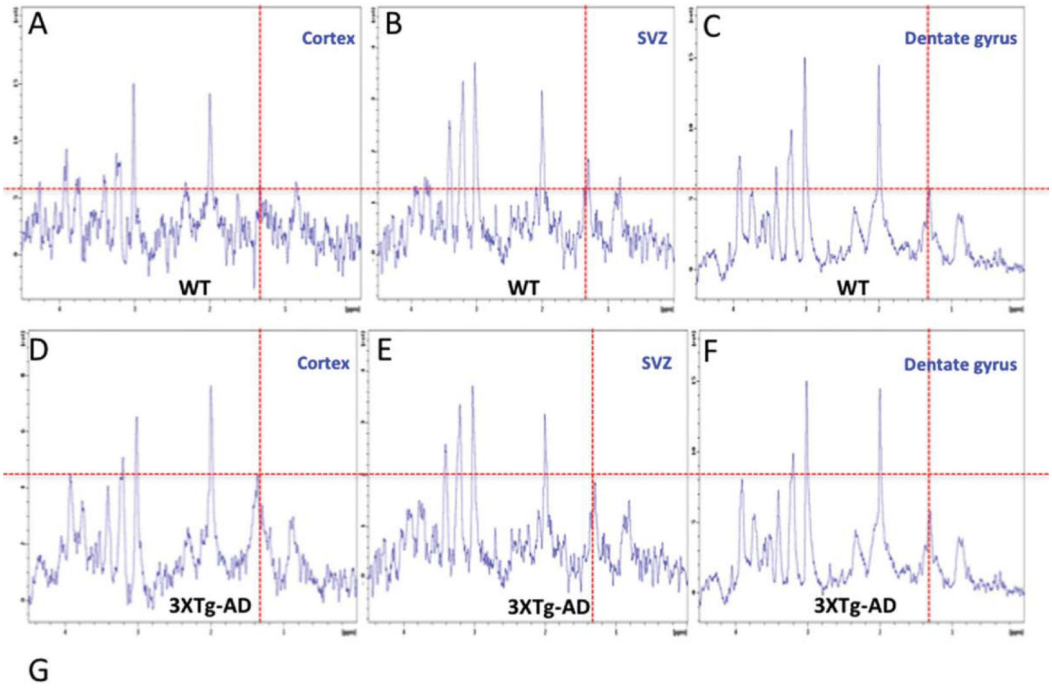

G

Lipid 1.28 ppm signal intensity as a ratio to Cr signal intensity in the mouse brain

	NTg	APP/PS1		NTg	3XTg-AD
DG	0.091	0.079		0.015	0.044
SVZ	0.298	1.074		0.048	0.075
Ctx	2.258	1.934		1.23	4.809

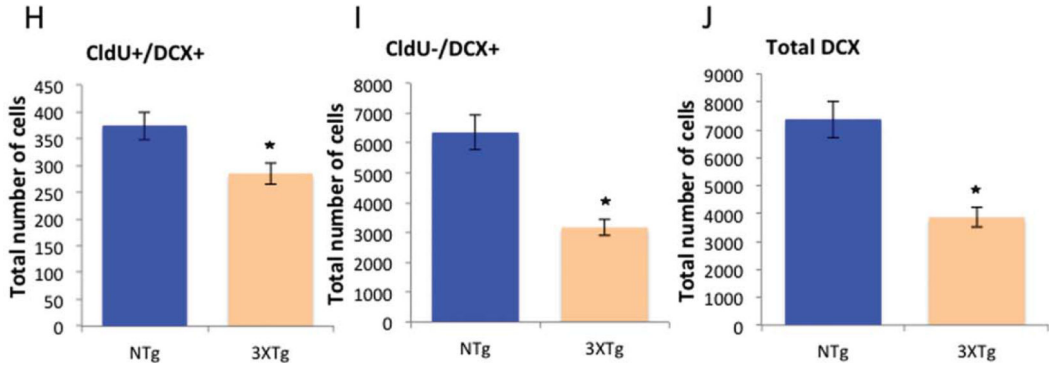

Fig. 3.

Level of the 1.28 ppm metabolite in the brains of 3XTg-AD mice. *In vivo* localized ^{1}H-MR spectra of mouse cortex (A, D), subventricular zone (B, E), and hippocampus (C, F) of wild type (A–C) and 3XTg-AD (D–F) mice. (G) Summary of level of the 1.28 ppm metabolite in the hippocampus (DG), subventricular zone (SVZ), and cortex (Ctx) of APPswe/PS1 ΔE9, 3XTg-AD and their corresponding wild type mice. (H–J) Extent of hippocampal neurogenesis in the 3XTg-AD mice and counterpart wild type. Graphs show the number of fast proliferating neuroblasts (CldU+DCX+; H), immature neurons (CldU−DCX+; I), and total DCX+ cells (J), as quantified by unbiased stereology.

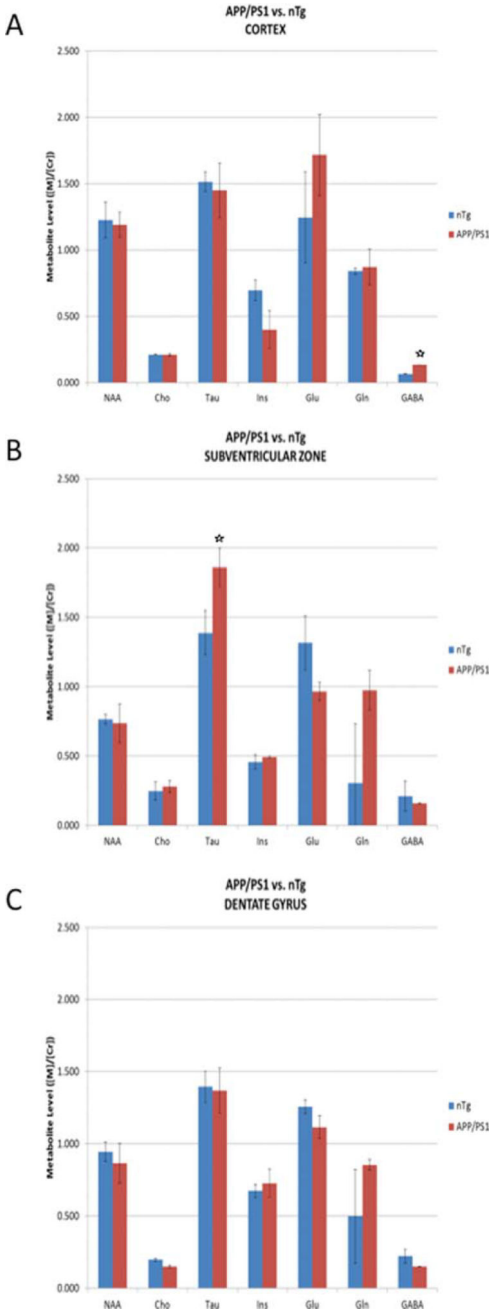

Fig. 4.

Level of metabolites in the ^{1}H-MR spectra of APPswe/PS1 ΔE9 mice. Level of metabolites in the cortex (A), subventricular zone (B), and the dentate gyrus of the hippocampus (C) of APPswe/PS1 ΔE9 (APP/PS1) and wild type (nTg) mice.

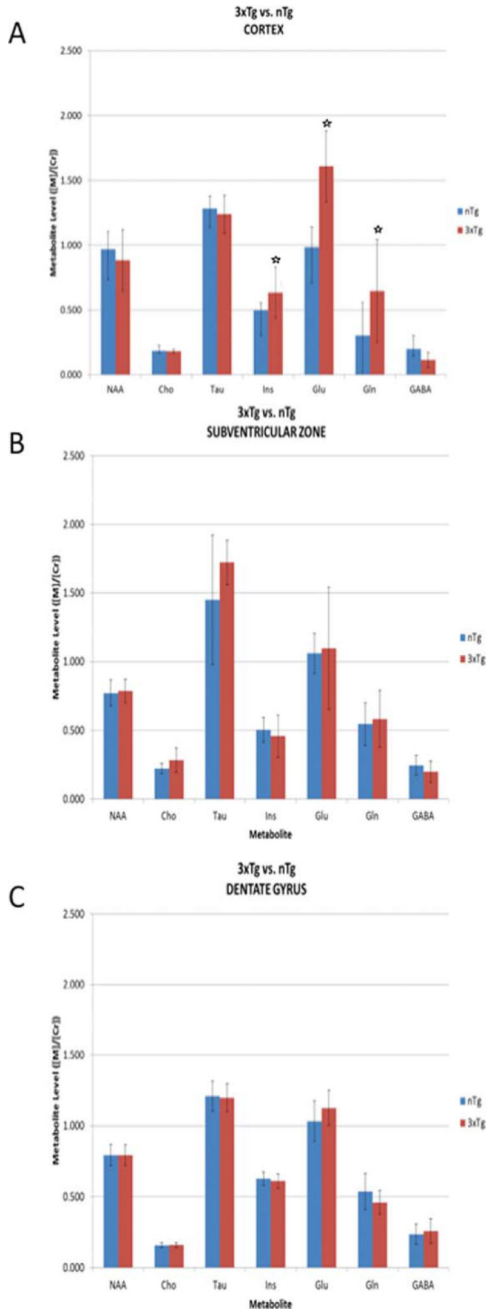

Fig. 5.

Metabolites in the ^{1}H-MR spectra of 3XTg-AD mice. Metabolites in the cortex (A), subventricular zone (B), and dentate gyrus of the hippocampus (C) of 3XTg-AD (3XTg) and wild type (nTg) mice.